Journal of Magnetism and Magnetic Materials 551 (2022) 169168

Contents lists available at ScienceDirect

Journal of Magnetism and Magnetic Materials

journal homepage: www.elsevier.com/locate/jmmm

Revisiting high-temperature phase transition and magnetocaloric effect of $LaFe_{11.6}Si_{1.4}$ alloy

Yuankui Yang [a], Kai Deng [a], Zhishuai Xu [a], Ke Han [b], Hongxing Zheng [a,*]

[a] Center for Advanced Solidification Technology, School of Materials Science and Engineering, Shanghai University, Shanghai 200444, China
[b] National High Magnetic Field Laboratory, Florida State University, Tallahassee 32310, FL, USA

ARTICLE INFO

Keywords:
Phase transformation
Heat treatment
Microstructure
Differential scanning calorimetry
Magnetocaloric alloys

ABSTRACT

Sufficient understanding on the formation mechanism of the $La(Fe,Si)_{13}$ phase (1:13 or τ_1) in La–Fe–Si alloys would be helpful in optimizing the parameters for high-temperature annealing. *In-situ* annealing experiments of a centrifugally as-cast $LaFe_{11.6}Si_{1.4}$ plate were performed by using a differential scanning calorimeter (DSC) in the present study. We confirmed that the τ_1 phase is resulted from a peritectic reaction between La-rich liquid phase and α(Fe) solid phase when isothermal annealing at 1423 K. A new finding of a eutectoid decomposition that may occur within the residual La-rich liquid phase upon cooling was revealed. The isothermal transformation kinetics of the τ_1 phase in the as-cast plate followed a simplified model of diffusion-controlled continuous network growth. The isothermal entropy change ($|\Delta S_M|$) was calculated using the Maxwell equation on $M-H$ data. The maximum $|\Delta S_M|$ value reached 26.89 J/(kg·K) under 30 kOe in the $LaFe_{11.6}Si_{1.4}$ sample annealed at 1423 K for 120 min.

1. Introduction

With the expanding concern for climate change, solid-state magnetic refrigeration is demonstrating extraordinary potential to replace gas-pressure refrigeration owing to its higher efficiency and environmentally friendly feature [1–3]. Several kinds of magnetocaloric candidate materials, including Gd–Si–Ge [4], Mn–Fe–(P,As) [5], La–Fe–Si [6,7], Heusler-type Ni–Mn–(Ga,In,Sn,Sb) [8,9] and Fe–Rh-based alloys [10,11], have been reported for the applications in the vicinity of room temperature. Among which, La–Fe–Si alloys are commercially promising due to non-toxic constituents, large relative cooling power and high thermal conductivity.

Firstly, plenty of efforts have been focused on the compositional adjustment through elemental alloying [12–22]. It was found that the Curie temperature of magnetic transition in La–Fe–Si alloys generally increases with expansion of the unit-cell and decreases with shrinkage although a few abnormal phenomena were reported [23]. Excluding the effect of impurities or secondary phases, it has been well accepted that the occupation site of external atoms in the $NaZn_{13}$-type crystal structure of $La(Fe,Si)_{13}$ phase (1:13 or τ_1) plays a crucial role [24]. Secondly, one realized that it is difficult to obtain high-proportional τ_1 phase in conventionally as-cast La–Fe–Si alloys [25], and the magnetic properties strongly depend on high-temperature annealing process [26]. For example, a pure τ_1 phase cannot be obtained in the arc-melted $LaFe_{11.6}Si_{1.4}$ ingot until it was annealed at 1373 K for 5 days [27]. The maximum isothermal entropy change (ΔS_M) of $LaFe_{11.5}Si_{1.5}$ melt-spun ribbons was 12 J/(kg·K) (H = 15 kOe) when annealing at 1273 K for 2 min, which strikingly enhanced to 17 J/(kg·K) when extending the annealing time to 120 min [28]. Lastly, although powder metallurgy [29,30], melt-spinning [31] and centrifugal casting [32] have been used for the production of La–Fe–Si alloy, it seems that annealing process is indispensable for the formation of high-proportional τ_1 phase.

Our previous work showed that centrifugal casting method is a promising approach to produce high-performance La–Fe–Si alloys [32], however, the understanding of the formation mechanism of the τ_1 phase was far from enough. As summarized in Ref. [33], Chen et al. [26] and Fu et al. [34] proposed that τ_1 phase formed through a peritectic reaction ($L_{La1Fe1Si1} + \alpha(Fe) \rightarrow \tau_1$) at 1531 K or through a eutectoid reaction ($La_1Fe_1Si_1 \rightarrow \tau_1 + La_5Si_3$) at 1402 K, respectively. Liu et al. [35] suggested that the formation may associate with a eutectoid reaction since they observed the transient-state α(Fe)/La-rich phase lamellar microstructure when annealing the $LaFe_{11.6}Si_{1.4}$ alloy at 1323 K. We recently noticed that similar lamellar microstructure in La-Fe-Si alloy was reported by Löwe et al. [36] and Yang et al. [37], however, the former

* Corresponding author.
E-mail address: hxzheng@shu.edu.cn (H. Zheng).

https://doi.org/10.1016/j.jmmm.2022.169168
Received 4 January 2022; Received in revised form 27 January 2022; Accepted 9 February 2022
Available online 14 February 2022

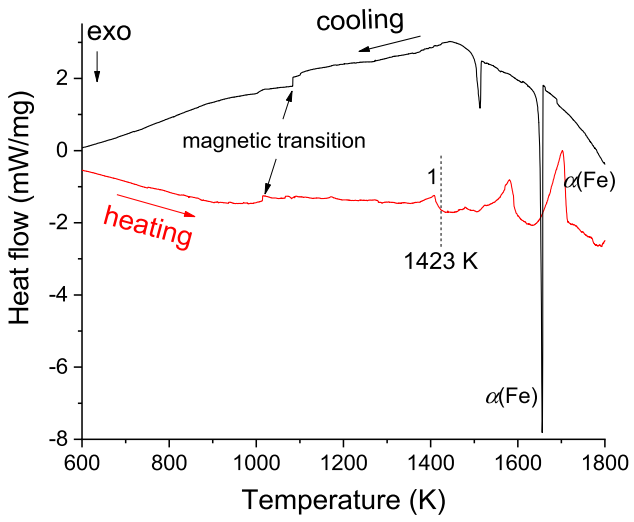

Fig. 1. DSC chart of the as-cast $LaFe_{11.6}Si_{1.4}$ sample. The magnetic transition of α(Fe) phase was identified by a small peak.

proposed that it was originated from the thermal decomposition of τ_1 phase and the latter attributed to a combination of disseverment processing and compositional re-homogenization between α(Fe) and La-rich phase. More controversial viewpoint on the phase transition behavior in La–Fe–Si alloys has been reported. For example, Kainuma et al. [27] determined the melting point of $La_1Fe_1Si_1$ phase to be 1553 K by DSC measurement, which is different from Chen et al. [26] that they suggested that the $La_1Fe_1Si_1$ solid phase melted at 1407 K. Therefore, it is necessary to revisit the phase transition behavior of La–Fe–Si alloy during high-temperature annealing process.

Different from conventional quartz-tube-sealing annealing method, a differential scanning calorimeter (DSC) was employed to a centrifugally as-cast solidified $LaFe_{11.6}Si_{1.4}$ sample so as to *in-situ* perform the annealing process at 1423 K. With a real-time recording on the heat-flow information [38], it was feasible to ensure that the transformation of τ_1 phase happened with the participation of a few liquid phase, and it is expected to explore a high-efficient annealing routine of La–Fe–Si alloy.

2. Materials and methods

A $LaFe_{11.6}Si_{1.4}$ (at.%) plate with a dimension of ~60 mm × 40 mm × 2.5 mm was fabricated using a self-designed centrifugal casting setup at a cooling rate of ~5000 K/s. The experimental details have been described elsewhere [32]. The obtained plate was then cut into small pieces with a diameter of 5 mm. Isothermal annealing experiments were performed using a differential scanning calorimeter (DSC, Netzsch 404 F3) in argon gas atmosphere. According to the differential scanning calorimetric chart (Fig. 1), a characteristic temperature of 1423 K, just above the first endothermic peak (1410 K) upon heating, was chosen to be the isothermal temperature in the present work. All as-cast $LaFe_{11.6}Si_{1.4}$ samples were heated to 1423 K at a rate of 20 K/min, holding for 0 min, 1 min, 5 min, 60 min and 120 min, respectively, and then cooled to room temperature at a rate of 20 K/min. The heat flow information during annealing processes was recorded (Fig. 2), showing good reproducibility.

Microstructural observation and elemental analysis were performed using an electron probe microanalyzer (EPMA-8050G, Shimadzu) equipped with a wavelength-dispersive spectrometer (WDS). The volume fractions of various constituent phases were determined based on the back-scattered electron images using Image Pro-Plus software. X-ray diffraction (DLMAX-2500) with Cu Kα radiation was employed to detect the phase and crystal structure. Magnetic properties were measured on a physical property measurement system (Quantum Design PPMS-9) under a maximum magnetic field up to 30 kOe.

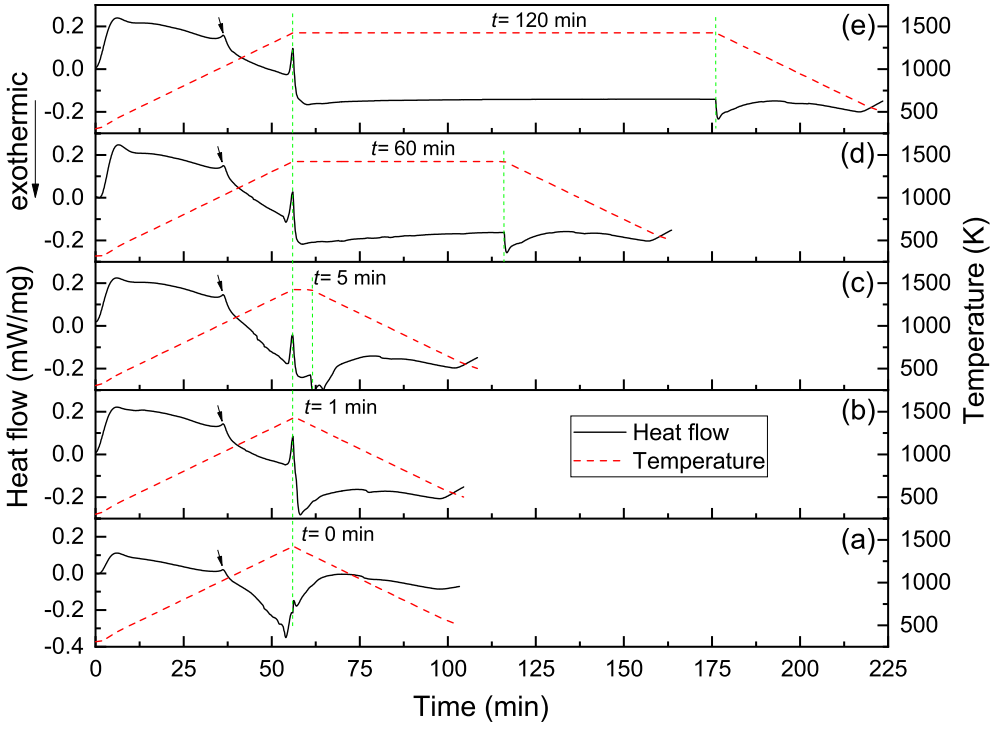

Fig. 2. Relationships of DSC heat flow (left vertical axis) and temperature (right vertical axis) *vs.* time for as-cast $LaFe_{11.6}Si_{1.4}$ samples with different isothermal annealing time (t) at 1423 K. (a) 0 min, (b) 1 min, (c) 5 min, (d) 60 min and (e) 120 min. The vertical dashed green lines indicate the start and finish of isothermal annealing at 1423 K. Black arrows on the heat flow curves at about 36 min indicates the magnetic transition of α(Fe) phase.

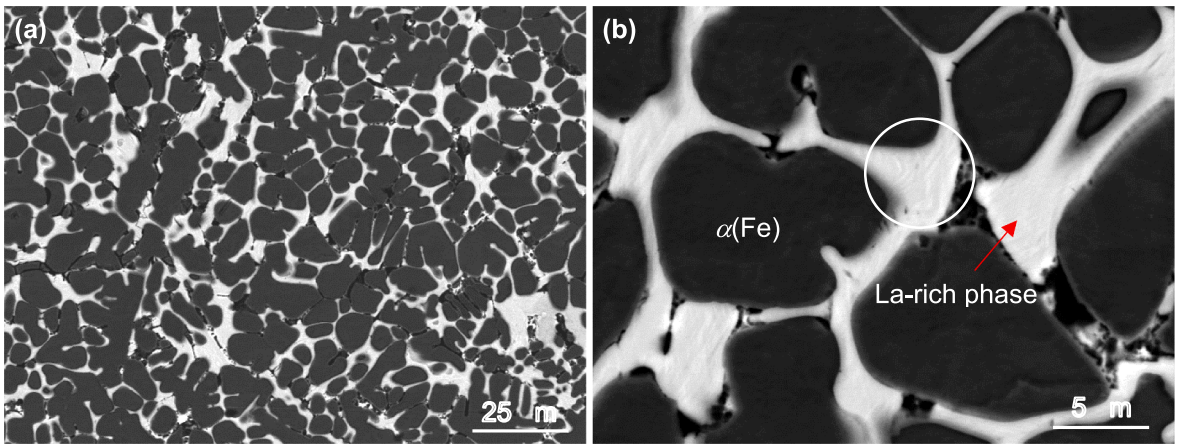

Fig. 3. SEM image of as-cast $LaFe_{11.6}Si_{1.4}$ sample (a). Enlarged image showing α(Fe) and La-rich phases (b).

Table 1
Compositional analyses of the $LaFe_{11.6}Si_{1.4}$ sample with different states (at.%).

	Region	La	Fe	Si	Phase
As-cast sample	White	31.26 ± 0.55	38.62 ± 0.76	30.12 ± 0.52	La-rich phase
	Black	0.50 ± 0.05	95.20 ± 0.17	4.30 ± 0.20	α(Fe)
Sample annealed for 0 min	White	34.10 ± 0.49	38.75 ± 0.42	27.46 ± 0.12	La-rich phase
	Black	0.93 ± 0.09	97.60 ± 0.08	1.45 ± 0.05	α(Fe)
	Grey	7.68 ± 0.06	85.92 ± 0.13	6.38 ± 0.12	τ_1
Sample annealed for 1 min	White	32.19 ± 0.41	37.78 ± 0.44	30.03 ± 0.33	La-rich phase
	Black	0.40 ± 0.02	97.34 ± 0.03	2.26 ± 0.04	α(Fe)
	Grey	6.71 ± 0.03	83.50 ± 0.24	9.79 ± 0.26	τ_1
Sample annealed for 5 min	white	32.83 ± 0.22	36.45 ± 0.44	30.72 ± 0.35	La-rich phase
	black	0.46 ± 0.02	97.25 ± 0.08	2.29 ± 0.07	α(Fe)
	grey	6.55 ± 0.07	83.47 ± 0.13	9.98 ± 0.12	τ_1
Sample annealed for 60 min	black	0.49 ± 0.02	96.95 ± 0.08	2.56 ± 0.08	α(Fe)
	grey	6.33 ± 0.02	83.75 ± 0.16	9.92 ± 0.16	τ_1
Sample annealed for 120 min	black	0.41 ± 0.02	97.14 ± 0.07	2.45 ± 0.08	α(Fe)
	grey	6.35 ± 0.08	83.83 ± 0.13	9.82 ± 0.20	τ_1

3. Results and discussion

3.1. High-temperature phase transition

The DSC heating curve showed that the melting occurred at 1706 K and magnetic transition of α(Fe) phase occurred at 1016 K (Fig. 1), as described in our previous work [32]. Black arrows as marked at about 36 min indicates the magnetic transition of α(Fe) phase (Fig. 2). The microscopy images showed homogeneously refined microstructure in the as-cast $LaFe_{11.6}Si_{1.4}$ plate (Fig. 3a). Enlarged SEM images showed dark α(Fe) grains surrounded by intermetallic compound networks in light contrast (Fig. 3b). WDS elemental analyses confirmed these dark grains represented α(Fe). Previous researchers have assumed that the white La-rich phase was $La_1Fe_1Si_1$ (1:1:1) [26–28,32–35], however, our WDS results did not fully support that assumption in the present work even though the uncertainty was considered. Different from conventional arc-melted alloys, the white La-rich phase contained more Fe element in the $LaFe_{11.6}Si_{1.4}$ plate produced by centrifugal casting method (see Table 1), which will be discussed later. As annealing at 1423 K increased up to 60 min, more La(Fe,Si)$_{13}$ phase (*i.e.* τ_1 phase) formed. Consequently, both black α(Fe) and white La-rich phase decreased significantly (Fig. 4). Between 60 min and 120 min, however, the white La-rich phase completely disappeared, and the other two phases remained almost level: the τ_1 matrix phase accounted for 97 vol %, and the isolated α(Fe) phase remained less than 3 vol%.

According to the XRD patterns obtained from the bulk samples (Fig. 5), one can see that most of the diffraction peaks can be well indexed to be either $NaZn_{13}$-type τ_1 phase or *bcc*-type α(Fe) phase. Three peaks at $2\theta = 24.70°$, 32.98° and 39.24° from $La_1Fe_1Si_1$ (Cu_2Sb-type structure) disappeared for the samples annealed at 1423 K for 60 min and 120 min. Additionally, three weak peaks at $2\theta = 21.34°$, 23.54° and 42.24° may be from $LaFe_xSi_{2-x}$ (AlB_2-type structure), $LaFeSi_2$ ($CeNiSi_2$-type structure) or $LaFe_2Si_2$ (Al_4Ba-type structure) in the samples annealed at 1423 K for 0 min and 1 min were detected [27], however, it is hard to distinguish these phases in Fig. 4 due to the rather small amount.

In order to quantitatively study the formation kinetics of the τ_1 phase in our sample, we measured the volume fraction of the τ_1 phase as a function of time subjected to isothermal annealing at 1423 K (Fig. 6). The volume fraction increased rapidly for the first two minutes (stage 1), slowly for the next 40 min (stage 2), and remained almost unchanged thereafter (stage 3). In the final stage, the volume fraction of the τ_1 phase remained the same, indicating that chemical homogenization may have occurred. From that behavior, we deduced that the formation kinetics of the τ_1 phase followed the JMAK equation [39–42]:

$$x(t) = 1 - exp(-k_v t^n)$$

where $x(t)$ is the fraction of the τ_1 phase after annealing for time t, and the two parameters characterizing the phase transition process are n (the Avrami index) and k_v (the formation rate constant). Using our experimental data, the values of n and k_v were determined to be 0.47 ± 0.03 and 0.69 ± 0.07 min^{-1}, respectively. When n is near 0.5, the formation of the phase can be visualized as the thickening of a very large plate (see Table 2) [43]. We used this simplified model to describe the formation of a phase as a continuous network growth. Dai et al. reported, during annealing at 1373 K of a $LaFe_{11.6}Si_{1.4}$ plate sealed in a quartz tube, that the n value was 0.43 [33], comparable to our present study although the transformation of τ_1 phase was completed within at least 48 h. In an arc-melted ingot of $La(Fe_{0.89}Si_{0.11})_{13}$, however, even with a chemical composition ($LaFe_{11.57}Si_{1.43}$) close to that of our centrifugally as-cast plate, the transformation of τ_1 phase required up to 200 h for isothermal annealing at 1323 K. The n value of the arc-melted-ingot was

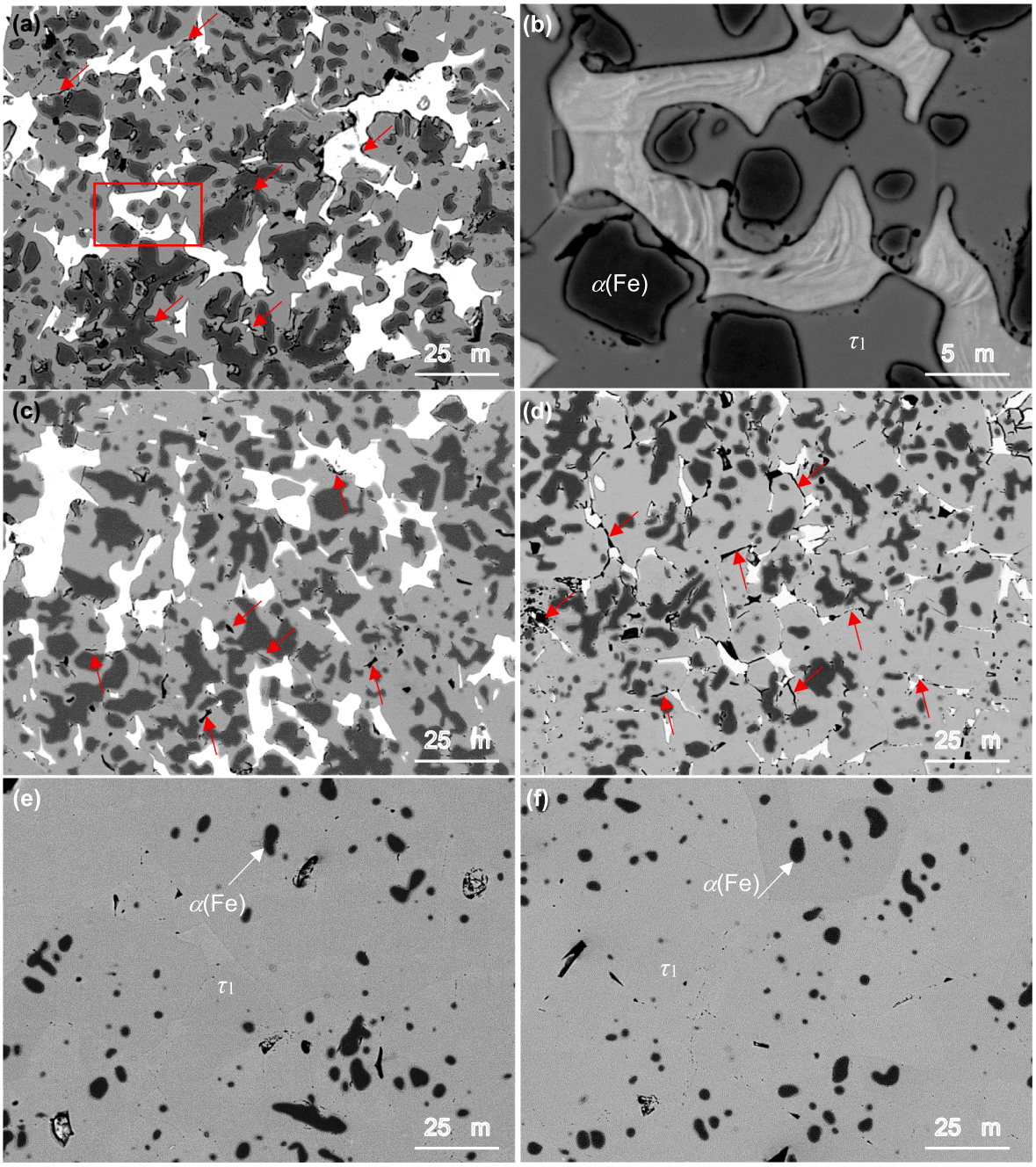

Fig. 4. SEM images of the $LaFe_{11.6}Si_{1.4}$ sample annealed at 1423 K for different isothermal time. (a,b) 0 min, (c) 1 min, (d) 5 min, (e) 60 min and (f) 120 min.

0.93, indicating that reaction in the arc-melted ingot followed the growth mechanism of a discontinuous τ_1 phase involving a finite long plate/needle [44].

The formation mechanism of τ_1 phase in $LaFe_{11.6}Si_{1.4}$ plate annealed at 1423 K was deduced from our microstructural data. Some microcracks were visible in Fig. 4a, c and d (as marked by red arrows) accompanying with the disappearance of a few white La-rich phase. It is reasonable to conclude that when annealing at 1423 K, above the first melting peak (1410 K), the τ_1 phase is resulted from a peritectic reaction between La-rich liquid phase and α(Fe) solid phase. There was almost no crack in the samples when annealing for 60 min and 120 min, indicating the peritectic reaction have completed. Enlarged SEM images for samples annealing at 1423 K for 1 min and 5 min (Fig. 7a and b) showed typical shell feature resulting from peritectic reaction. From the elemental distributions of La, Fe and Si in the sample annealing for 1 min (Fig. 7c-e), one can see a narrow transition layer between white La-rich phase and grey τ_1 phase (as marked by red arrows in Fig. 7c), indicating the occurrence of strong atomic interdiffusion. After the La-rich liquid phase was consumed, the formation of τ_1 phase enters solid-state compositional homogenization. In accordance with our previous study [32], the endothermic peaks at 1477 K and 1581 K correspond to the formation and remelting of τ_1 phase upon heating, respectively.

Lastly, it should be noted that the white La-rich phase has been assumed to be $La_1Fe_1Si_1$ phase, however, the compositional analyses (Table 1) in the present study do not fully support the point. From the enlarged image (Fig. 4b) taken from the red rectangular frame in Fig. 4a, one can clearly distinguish two distinct phases existed in the white region when the sample was heated to 1423 K and then cooling directly (t = 0 min). Furthermore, lamellar feature can also be observed in the residual white phase for the samples when holding for 1 min and 5 min

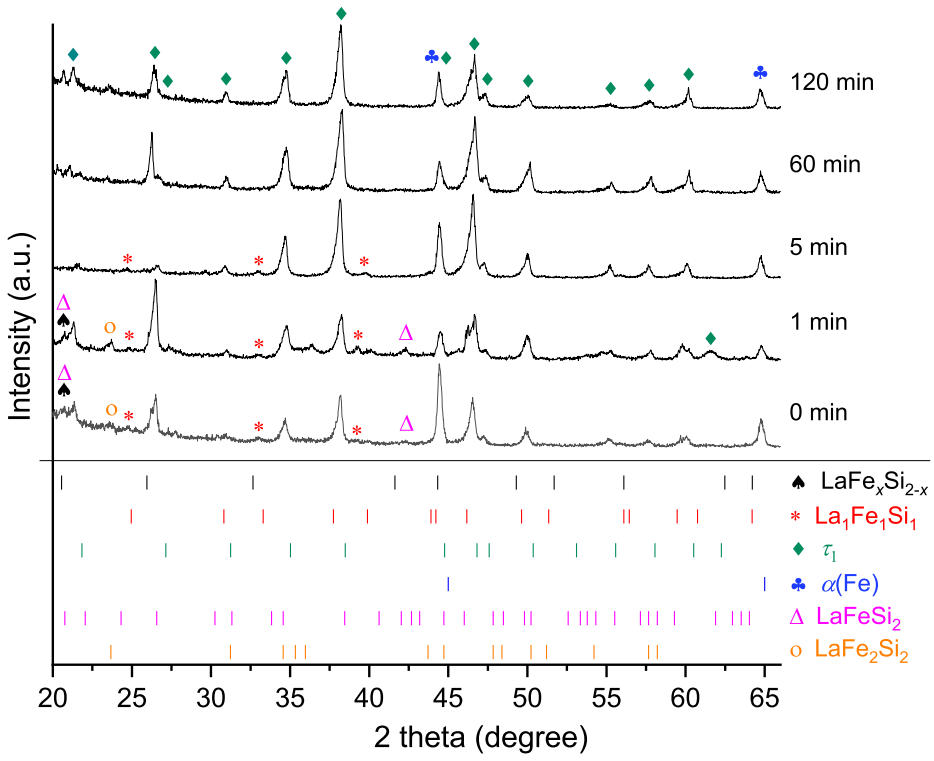

Fig. 5. XRD patterns of the $LaFe_{11.6}Si_{1.4}$ sample annealed at 1423 K for different isothermal time.

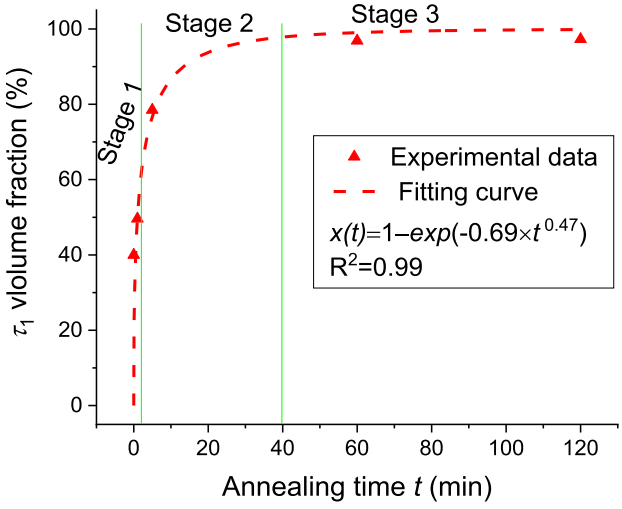

Fig. 6. Volume fraction of τ_1 phase as a function of isothermal annealing time at 1423 K for the $LaFe_{11.6}Si_{1.4}$ sample.

Table 2
Summary of the n values in kinetic law $x(t) = 1 - exp(-k_v t^n)$ during diffusion-controlled growth process corresponding to various experimental conditions [43].

	n
All shapes growing from small dimensions	>1.5
Growth of particles of appreciable initial volume	1 ~ 1.5
Needles and plates of finite long dimensions	1
Thickening of long cylinders (needles)	1
Thickening of very large plates	0.5

(Fig. 7a and b), which can be reflected by the brightness contrast from the back-scattered electron images. Blurred lamellar feature also appeared in the centrifugally as-cast sample, as marked by a white circle in Fig. 3b. The compositional difference is beyond the detection limit of WDS instrument, however, in combination with the XRD results, we can still speculate that the La-rich liquid phase may undergo a eutectoid decomposition upon cooling, for example, $L_{La} \rightarrow La_1Fe_1Si_1 + LaFe_xSi_{2-x}$ or other phases.

3.2. Magnetic properties

A magnetization curve as a function of temperature ($M-T$) for the $LaFe_{11.6}Si_{1.4}$ sample annealed for 120 min was measured under a low magnetic field of 500 Oe. One can find that the sample changed from ferromagnetic to paramagnetic on heating (Fig. 8a) [45]. The non-zero magnetization (2.5 emu/g) above the Curie temperature was associated with the residual of a few α(Fe) phase (Fig. 4f).

Isothermal magnetization curves ($M-H$) around the magnetic transition between 150 K and 240 K were measured (Fig. 8b). In the present study, all magnetization isothermals were recorded in the following sequence: when the sample was initially cooled to 150 K under a zero-field, the magnetic field was gradually increased from zero to a maximum strength of 30 kOe and then decreased to zero. After one $M-H$ curve was measured, the temperature was raised to the next consecutive value at an interval of 3 K. When the temperature was lower than 189 K, the sample showed ferromagnetism. Between 189 K and 198 K, hysteresis losses (HL) were clear. The hysteresis loss of energy generally dissipates in the form of thermal energy, and thus lead to the decrease of refrigeration capacity. Further raising the temperature up to 201 K, the sample fully transformed to be paramagnetic state. The Arrot plots converted from the $M-H$ curves showed typical S-shape around the Curie temperature (Fig. 9). According to Inoue-Shimizu model [46], the slope should be all positive if the type of phase transition is second-order, and the curve should have a negative slope (S-shape) if the type is first-order. We therefore conclude that the annealed sample underwent a first-order phase transition in the vicinity of 192 K.

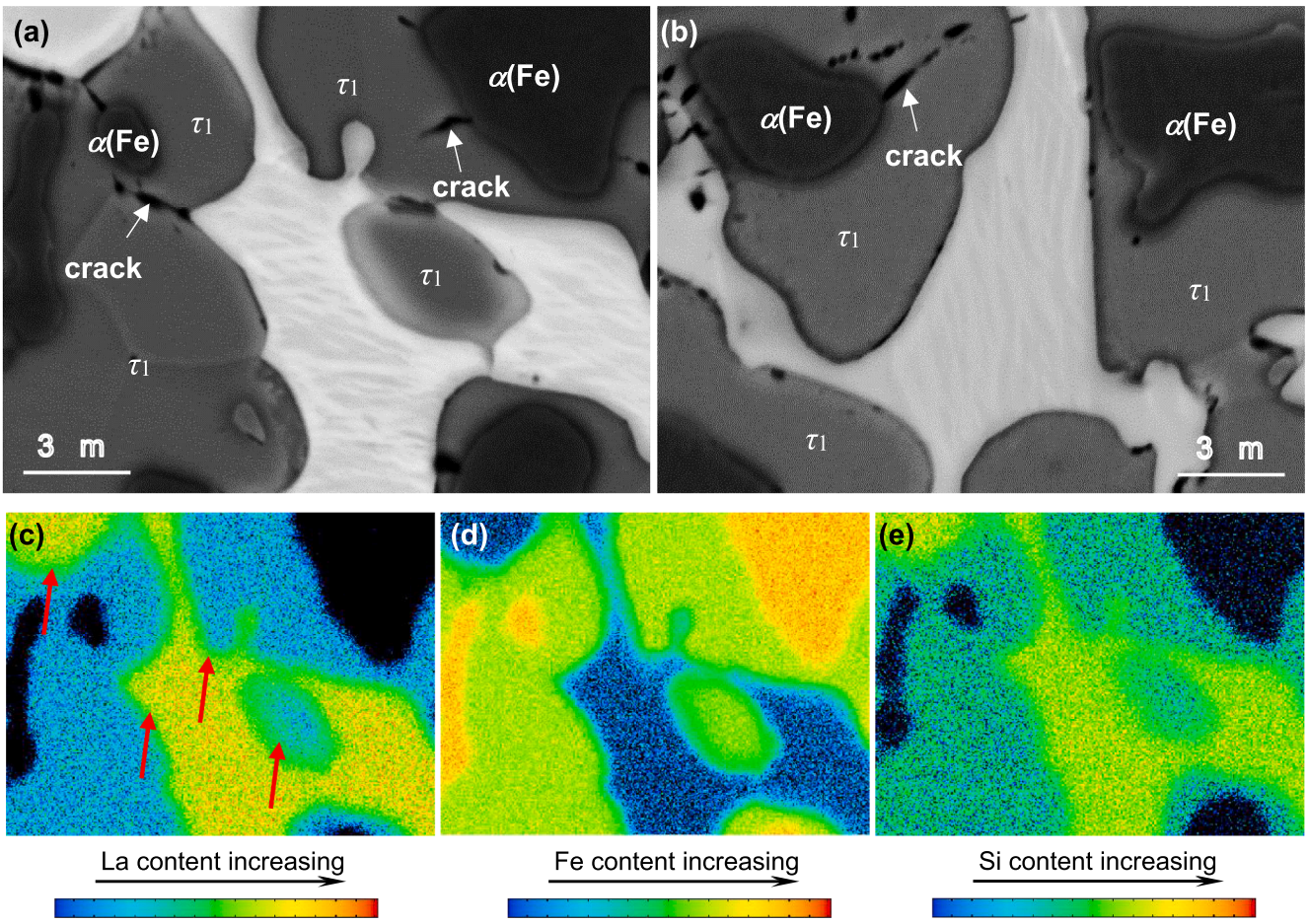

Fig. 7. Enlarged SEM images of the $LaFe_{11.6}Si_{1.4}$ sample annealed at 1423 K for 1 min (a) and 5 min (b). (c-e) showing the elemental distributions of La, Fe and Si, respectively, corresponding to (a).

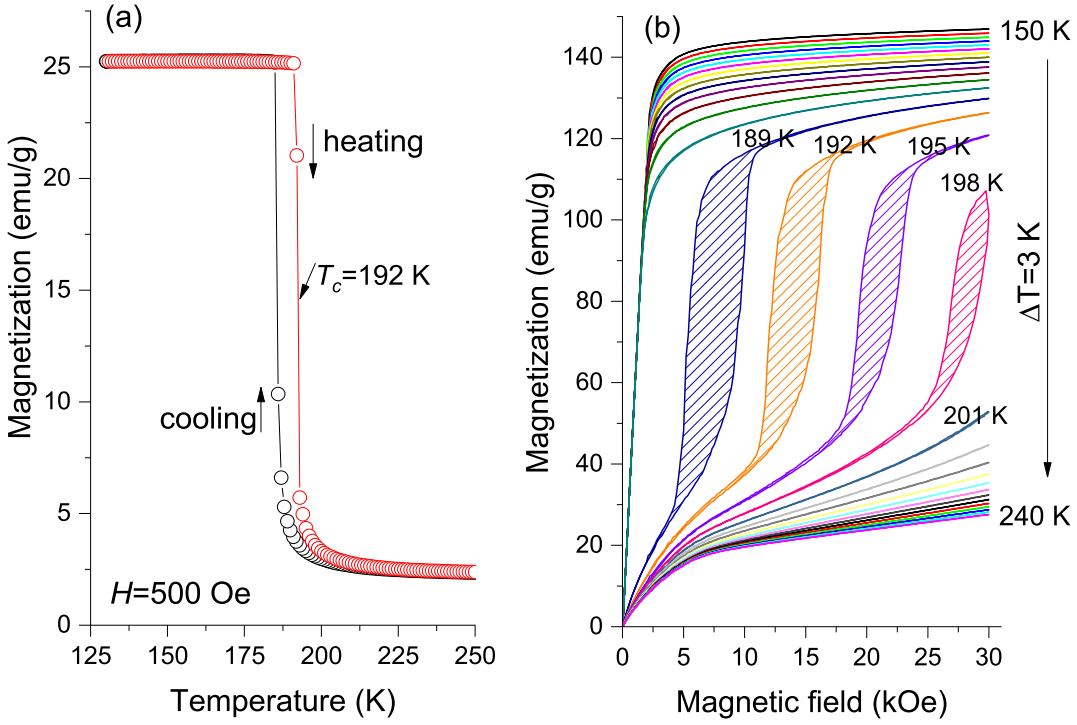

Fig. 8. (a) Magnetization curve ($M-T$) of the $LaFe_{11.6}Si_{1.4}$ sample annealed at 1423 K for 120 min under a magnetic field of 500 Oe. (b) Isothermal magnetization curves ($M-H$) measured between 150 K and 240 K under a magnetic field change of 30 kOe. The strips in (b) indicate hysteresis loss.

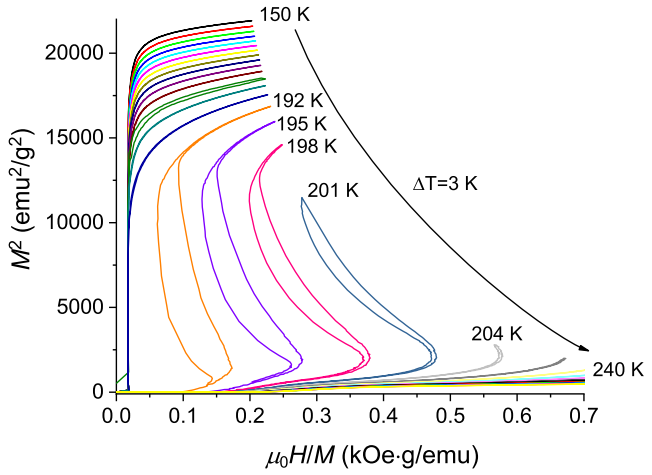

Fig. 9. The Arrot plots of the $LaFe_{11.6}Si_{1.4}$ sample annealed at 1423 K for 120 min.

Isothermal entropy change (ΔS_M) is a key parameter to evaluate refrigeration capacity, which can be estimated using the Maxwell equation in the present work:[47]

$$\Delta S_M(T,H) = S(T,H) - S(T,0) = \int_0^H \left(\frac{\partial M}{\partial T}\right)_H dH.$$

The ΔS_M peaks of our sample showed asymmetrical broadening phenomena at higher temperatures (Fig. 10a). The corresponding average hysteresis loss was also used for estimation of refrigeration capacity by finding the integral of *HL* with respect to a temperature within the temperature range of magnetic transition (Fig. 10b). By comprehensively considering both ΔS_M and *HL*, effective refrigeration capacity (RC_{eff}) can be calculated as follows:

$$RC_{eff} = \int_{T_{cold}}^{T_{hot}} |\Delta S_M(T)| dT - \int_{T_{cold}}^{T_{hot}} HL(T) dT / (T_{hot} - T_{cold}),$$

where T_{hot} and T_{cold} are the temperatures corresponding to the full-width-half-minimum (FWHM) of the isothermal entropy curve (see Table 3). Compared to our previous work [32], the RC_{eff} value slightly increased (8.5%) and the annealing time shortened from 180 min to 120 min, which is closely linked to the accelerated transformation by increasing the annealing temperature from 1373 K to 1423 K. Combining optimized heat treatment with the centrifugal casting method, the refrigeration capacity was comparable to the conventionally arc-melted $LaFe_{11.6}Si_{1.4}$ sample annealed at 1523 K for 4 h [48].

4. Conclusions

With regard to the $LaFe_{11.6}Si_{1.4}$ plate produced by centrifugal casting method, the high-temperature phase transition behavior was revisited. *In-situ* annealing process was performed by using a differential scanning calorimeter. After analyzing the magnetic properties of samples cut from the as-cast plate and annealed at 1423 K for 120 min, we drew the following conclusions:

(1) The τ_1 phase was confirmed to form through a peritectic reaction between La-rich liquid phase and α(Fe) phase in samples isothermally annealed at 1423 K. The white La-rich phase in the

Table 3
Magnetic properties of the $LaFe_{11.6}Si_{1.4}$ sample annealed at 1423 K for 120 min.

H (kOe)	T_{cold} (K)	T_{hot} (K)	$\lvert\Delta S_M\rvert$ (J/(kg·K))	RC_{eff} (J/kg)
10	187.40	190.83	23.40	55.63
20	187.32	194.57	26.12	132.75
30	187.30	199.08	26.89	227.10

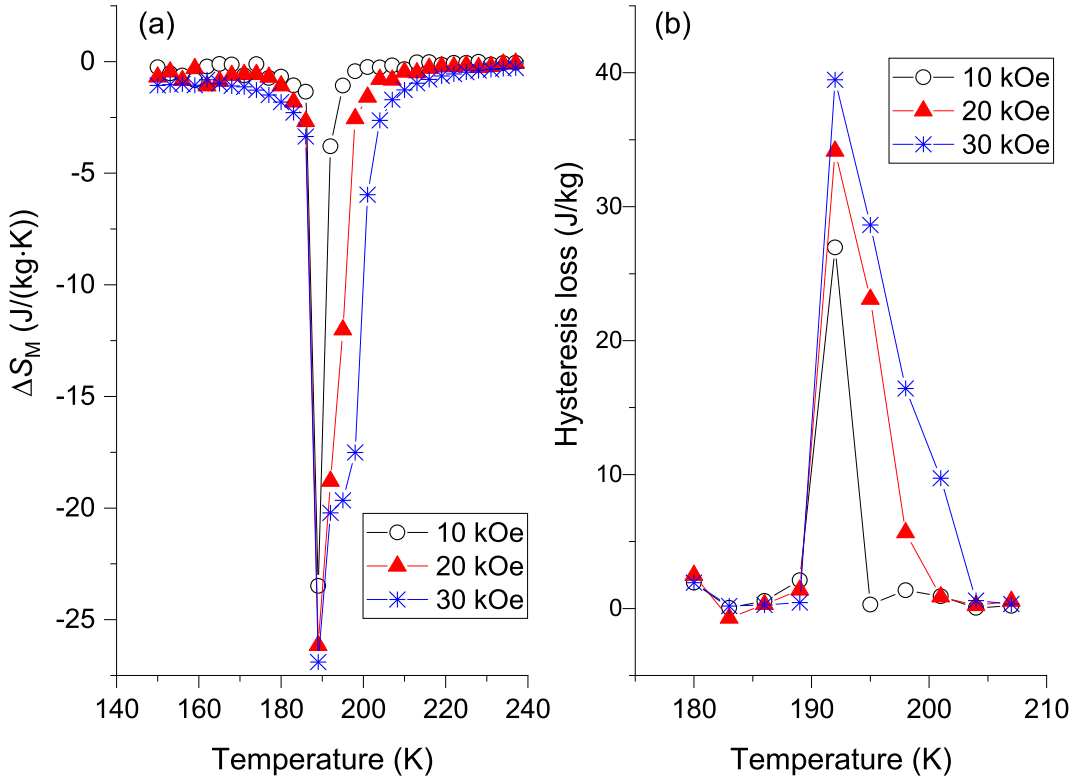

Fig. 10. Isothermal entropy change (ΔS_M) as a function of temperature for the $LaFe_{11.6}Si_{1.4}$ sample annealed at 1423 K for 120 min (a) and the corresponding hysteresis losses (b) under the magnetic field change of 10 kOe, 20 kOe and 30 kOe, respectively.

centrifugally as-cast plate may undergo a eutectoid decomposition upon cooling.

(2) The formation kinetics of the τ_1 phase in the as-cast $LaFe_{11.6}Si_{1.4}$ plate followed a simplified model of one-dimensional diffusion-controlled continuous network growth. Using the Maxwell equation on $M-H$ data, a maximum $|\Delta S_M|$ value of 26.89 J/(kg·K) under 30 kOe was achieved in the $LaFe_{11.6}Si_{1.4}$ sample annealed at 1423 K for 120 min.

Declaration of Competing Interest

The authors declare that they have no known competing financial interests or personal relationships that could have appeared to influence the work reported in this paper.

Acknowledgements

The authors gratefully acknowledge the financial support of the National Natural Science Foundation of China (51904182 and 52074180). A portion of this work was performed at the National High Magnetic Field Laboratory (NHMFL), which is supported by the National Science Foundation (DMR-1644779) and the State of Florida. The authors thank Mary Tyler for editing.

References

[1] L.W. Li, M. Yan, Recent progresses in exploring the rare earth based intermetallic compounds for cryogenic magnetic refrigeration, J. Alloys Compd. 823 (2020) 153810.
[2] N.T.M. Duc, H.X. Shen, E.M. Clements, O. Thiabgoh, M.H. Phan, J.L.S. Llamazares, Enhanced refrigerant capacity and Curie temperature of amorphous $Gd_{60}Fe_{20}Al_{20}$ micro-wires, J. Alloys Compd. 807 (2019) 151694.
[3] V. Franco, J.S. Blázquez, J.J. Ipus, J.Y. Law, L.M. Moreno-Ramírez, A. Conde, Magnetocaloric effect: from materials research to refrigeration devices, Prog. Mater. Sci. 93 (2018) 112–232.
[4] V.M. Andrade, J.H. Belo, N.R. Checca, A. Rossi, F. Garcia, B. Almeida, J.C. G. Tedesco, A. Poulain, A.M. Pereira, M.S. Reis, J.P. Araújo, Unit cell volume reduction of $Gd_5(Si,Ge)_4$ nanoparticles controlled by bulk compressibility, J. Alloys Compd. 849 (2020) 156384.
[5] C.F. Li, Z.G. Zheng, W.H. Wang, J.Y. Liu, L. Lei, D.C. Zeng, Effect of M/NM ratios on structural and magnetic properties of $(Mn,Fe)_2(P,Si)$ compounds, Phys. B 594 (2020) 412309.
[6] H. Zhang, M. Zhang, Y.Y. Shao, L.H. Zhu, J. Liu, Microstructure and magnetocaloric properties of non-stoichiometric $La_{1.5}Fe_{12.2-x}Co_{0.8}Si_x$ alloys, J. Alloys Compd. 720 (2017) 432436.
[7] S.M. Wu, X.C. Zhong, X.T. Dong, C.L. Liu, J.H. Huang, Y.L. Huang, H.Y. Yu, Z. W. Liu, Y.S. Huang, R.V. Ramanujan, $LaFe_{11.6}Si_{1.4}/Pr_{40}Co_{60}$ magnetocaloric composites for refrigeration near room temperature, J. Alloys Compd. 10 (2021) 159796.
[8] Y. Zhang, S.V. Kumar, W.W. Xiang, Z.G. Wu, Z.Y. Sun, Martensitic transformation and mechanical properties of grain refined Ni–Co–Mn–Sn Heusler alloys *via* Cr doping, Mater. Sci. Eng. A 804 (2021) 140777.
[9] H.L. Wang, D. Li, G.Y. Zhang, Z.B. Li, B. Yang, H.L. Yan, D.Y. Cong, C. Esling, X. Zhao, L. Zuo, Highly sensitive elastocaloric response in a directionally solidified $Ni_{50}Mn_{33}In_{15.5}Cu_{1.5}$ alloy with strong $<001>_A$ preferred orientation, Intermetallics 140 (2022) 107379.
[10] R.R. Gimaev, A.A. Vaulin, A.F. Gubkin, V.I. Zverev, Peculiarities of magnetic and magnetocaloric properties of Fe–Rh alloys in the range of antiferromagnet–ferromagnet transition, Phys. Metals Metallogr. 121 (2020) 823–850.
[11] A.S. Komlev, D.Y. Karpenkov, D.A. Kiselev, T.S. Ilina, A. Chirkova, R.R. Gimaev, T. Usami, T. Taniyama, V.I. Zverev, N.S. Perov, Ferromagnetic phase nucleation and its growth evolution in FeRh thin films, J. Alloys Compd. 874 (2021) 159924.
[12] Y.M. Zhu, K. Xie, X.P. Song, Z.B. Sun, W.P. Lv, Magnetic phase transition and magnetic entropy change in melt-spun $La_{1-x}Nd_xFe_{11.5}Si_{1.5}$ ribbons, J. Alloys Compd. 392 (2005) 20–23.
[13] S. Fujieda, A. Fujita, K. Fukamichi, N. Hirano, S. Nagaya, Large magnetocaloric effects enhanced by partial substitution of Ce for La in $La(Fe_{0.88}Si_{0.12})_{13}$ compound, J. Alloys Compd. 408 (2006) 1165–1168.
[14] H. Zhang, J. Shen, Z.Y. Xu, X.Q. Zheng, F.X. Hu, J.R. Sun, B.G. Shen, Simultaneous enhancements of Curie temperature and magnetocaloric effects in the $La_{1-x}Ce_xFe_{11.5}Si_{1.5}C_y$ compounds, J. Magn. Magn. Mater. 324 (2012) 484–487.
[15] J.J. Liu, Y. Zhang, J. Zhang, W.X. Xia, A.R. Yan, Systematic study of the microstructure and magnetocaloric effect of bulk and melt-spun ribbons of La–Pr–Fe–Si compounds, J. Magn. Magn. Mater. 350 (2014) 94–99.
[16] P. Gębara, M. Cesnek, J. Bednarcik, Anomalous behavior of thermal expansion of α-Fe impurities in the $La(Fe,Co,Si)_{13}$-based alloys modified by Mn or selected lanthanides (Ce,Pr,Ho), Curr. Appl. Phys. 19 (2019) 188–192.
[17] L.M. Moreno-Ramírez, C. Romero-Muñiz, J.Y. Law, V. Franco, A. Conde, I. A. Radulov, F. Maccari, K.P. Skokov, O. Gutfleisch, The role of Ni in modifying the order of the phase transition of $La(Fe,Ni,Si)_{13}$, Acta Mater. 160 (2018) 137–146.
[18] M.M. Din, J.L. Wang, R. Zeng, P. Shamba, J.C. Debnath, S.X. Dou, Effects of Cu substitution on structural and magnetic properties of $La_{0.7}Pr_{0.3}Fe_{11.4}Si_{1.6}$ compounds, Intermetallics 36 (2013) 1–7.
[19] H.N. Bez, B.G.F. Eggert, J.A. Lozano, C.R.H. Bahl, J.R. Barbosa, C.S. Teixeira, P.A. P. Wendhausen, Magnetocaloric effect and H gradient in bulk $La(Fe,Si)_{13}H_y$ magnetic refrigerants obtained by HDSH, J. Magn. Magn. Mater. 386 (2015) 125–128.
[20] M. Piazzi, C. Bennati, C. Curcio, M. Kuepferling, V. Basso, Modeling specific heat and entropy change in La(Fe–Mn–Si)$_{13}$–H compounds, J. Magn. Magn. Mater. 400 (2016) 349–355.
[21] X. Chen, Y.G. Chen, Y. Tang, Phase, structural, and magnetocaloric properties of high temperature annealed $LaFe_{11.6}Si_{1.4}B_x$, J. Alloys Compd. 509 (2011) 2864–2869.
[22] W. Wei, R.G. Huang, H.L. Dai, Y. Shan, Y.Q. Zhao, S.B. Guo, C.J. Huang, L.F. Li, Tunable near-zero thermal expansion in the C-doped $La(Fe,Si)_{13}$ compounds at cryogenic temperatures, Mater. Lett. 237 (2019) 26–28.
[23] D.T. Kim Anh, N.P. Thuy, N.H. Duc, T.T. Nhien, N.V. Nong, Nong, Magnetism and magnetocaloric effect in $La_{1-y}Nd_y(Fe_{0.88}Si_{0.12})_{13}$ compounds, J. Magn. Magn. Mater. 262 (2003) 427–431.
[24] L. Jia, J.R. Sun, J. Shen, B. Gao, T.Y. Zhao, H.W. Zhang, F.X. Hu, B.G. Shen, Influence of interstitial and substitutional atoms on the crystal structure of La(Fe, $Si)_{13}$, J. Alloys Compd. 509 (2011) 5804–5809.
[25] H. Zhang, B. Bao, P.J. Shi, B. Fu, Y. Long, Y.Q. Chang, F.R. Wan, Phase formation with $NaZn_{13}$ structure in metamagnetic $La(Fe_{1-x}Co_x)_{11.9}Si_{1.1}$ compounds, J. Rare Earths 26 (2008) 727–730.
[26] C. Xiang, Y.G. Chen, Y. Tang, High-temperature phase transition and magnetic property of $LaFe_{11.6}Si_{1.4}$ compound, J. Alloys Compd. 509 (2011) 8534–8541.
[27] K. Niitsu, R. Kainuma, Phase equilibria in the Fe–La–Si ternary system, Intermetallics 20 (2012) 160–169.
[28] X.L. Hou, L. Paula, Y. Kelley, C.Y. Xue, H. Liu, N. Xu, C.W. Han, H. Ma, M. H. Srikanth, Phan, Formation mechanisms of $NaZn_{13}$-type phase in giant magnetocaloric La–Fe–Si compounds during rapid solidification and annealing, J. Alloys Compd. 646 (2015) 503–511.
[29] B. Rosendahl Hansen, L. Theil Kuhn, C.R.H. Bahl, M. Lundberg, C. Ancona-Torres, M. Katter, Properties of magnetocaloric $La(Fe,Co,Si)_{13}$ produced by powder metallurgy, J. Magn. Magn. Mater. 322 (2010) 3447–3454.
[30] X.C. Zhong, X.L. Feng, X.W. Huang, X.Y. Shen, Z.W. Liu, Structure and magnetocaloric effect of $La_{0.7}Ce_{0.3}(Fe_{0.92}Co_{0.08})_{11.4}Si_{1.6}$ bulk alloy prepared by powder metallurgy, J. Alloys Compd. 685 (2016) 913–916.
[31] Y. Jian, Y.Y. Shao, Z.X. Feng, J. Liu, The effect of cooling rate on the phase formation and magnetocaloric properties in $La_{0.6}Ce_{0.4}Fe_{11.0}Si_{2.0}$ alloys, J. Magn. Magn. Mater. 452 (2018) 473–476.
[32] Z.S. Xu, Y.T. Dai, Y. Fang, Z.P. Luo, K. Han, C.J. Song, Q.J. Zhai, H.X. Zheng, High-temperature phase transition behavior and magnetocaloric effect in a sub-rapidly solidified La–Fe–Si plate produced by centrifugal casting, J. Mater. Sci. Technol. 34 (2018) 1337–1343.
[33] Y.T. Dai, Z.S. Xu, Z.P. Luo, K. Han, Q.J. Zhai, H.X. Zheng, Phase formation kinetics, hardness and magnetocaloric effect of sub-rapidly solidified $LaFe_{11.6}Si_{1.4}$ plates during isothermal annealing, J. Magn. Magn. Mater. 454 (2018) 356–361.
[34] S. Fu, Y. Long, Y.Y. Sun, J. Hu, Microstructural evolution and phase transition dependent on annealing temperature and carbon content for $LaFe_{11.5}Si_{1.5}C_x$ compounds prepared by arc-melting, Intermetallics 39 (2013) 79–83.
[35] L. Jian, M. Krautz, K. Skokov, T.G. Woodcock, O. Gutfleisch, Systematic study of the microstructure, entropy change and adiabatic temperature change in optimized La–Fe–Si alloys, Acta Mater. 59 (2011) 3602–3611.
[36] K. Löwe, J. Liu, K. Skokov, J.D. Moore, H. Sepehri-Amin, K. Hono, M. Katter, O. Gutfleisch, The effect of the thermal decomposition reaction on the mechanical and magnetocaloric properties of $La(Fe,Si,Co)_{13}$, Acta Mater. 60 (2012) 4268–4276.
[37] D.M. Stefanescu, R. Suarez, S.B. Kim, 90 years of thermal analysis as a control tool in the melting of cast iron, China Foundry 17 (2020) 69–84.
[38] L. Yang, Z. Zhou, S. Feng, J.H. Li, J. Liu, J. Li, Q.D. Hu, J.G. Li, Microstructure and magnetic property of $LaFe_{11.6}Si_{1.4}$ magnetocaloric alloys by a novel short time heat treatment, Intermetallics 105 (2019) 1–5.
[39] W.A. Johnson, R.F. Mehl, Reaction kinetics in processes of nucleation and growth, Trans. AIME 135 (1939) 416–458.
[40] M. Avrami, Kinetics of phase change: I. General theory, J. Phys. Chem. 7 (1939) 1103.
[41] M. Avrami, Kinetics of phase change: II. Transformation-time relations for random distribution of nuclei, J. Chem. Phys. 8 (1940) 212–224.
[42] A.N. Kolmogorov, On the statistical theory of crystallization of metals, Bull. Acad. Sci. USSR Math. Ser. 1 (1937) 355–359.
[43] J.W. Christain, The Theory of Transformations in Metals and Alloys: I. Equilibrium and General Kinetic Theory, Pergamon Press, Oxford, 1975.
[44] S. Fujieda, K. Fukamichi, S. Suzuki, Microstructure and isothermal magnetic entropy change of $La(Fe_{0.89}Si_{0.11})_{13}$ in a single-phase formation process by annealing, J. Alloys Compd. 566 (2013) 196–200.
[45] P. Shamb, R. Zeng, J.L. Wang, S.J. Campbell, S.X. Dou, Enhancement of the refrigerant capacity in low level boron doped $La_{0.8}Gd_{0.2}Fe_{11.4}Si_{1.6}$, J. Magn. Magn. Mater. 331 (2013) 102–108.

[46] N.H. Dung, L. Zhang, Z.Q. Ou, E. Brück, From first-order magneto-elastic to magneto-structural transition in $(Mn,Fe)_{1.95}P_{0.50}Si_{0.50}$ compounds, Appl. Phys. Lett. 99 (2011) 092511.
[47] M. Földeàki, R. Chahine, T.K. Bose, Magnetic measurements: A powerful tool in magnetic refrigerator design, J. Appl. Phys. 77 (1995) 3528–3537.
[48] X. Chen, Y.G. Chen, Y.B. Tang, The influence of different cooling processes on phase, microstructure, and magnetocaloric properties of $LaFe_{11.6}Si_{1.4}$ compounds, Solid State Commun. 186 (2016) 56–63.